THE JOURNAL OF PHYSICAL CHEMISTRY A
A JOURNAL OF THE AMERICAN CHEMICAL SOCIETY

pubs.acs.org/JPCA
Article

Comparing Density Functional Theory Metal–Ligand Bond Dissociation Enthalpies with Experimental Solution-Phase Enthalpies of Activation for Bond Dissociation

Published as part of The Journal of Physical Chemistry A virtual special issue "Krishnan Raghavachari Festschrift".

Edward N. Brothers,* Ashfaq A. Bengali, Giovanni Scalmani, Benjamin G. Janesko, Pragya Verma, Donald G. Truhlar, and Michael J. Frisch

Cite This: *J. Phys. Chem. A* 2023, 127, 9695–9704
Read Online

ABSTRACT: The predictive ability of density functional theory is fundamental to its usefulness in chemical applications. Recent work has compared solution-phase enthalpies of activation for metal–ligand bond dissociation to enthalpies of reaction for bond dissociation, and the present work continues those comparisons for 43 density functional methods. The results for ligand dissociation enthalpies of 30 metal–ligand complexes tested in this work reveal significant inadequacies of some functionals as well as challenges from the dispersion corrections to some functionals. The analysis presented here demonstrates the excellent performance of a recent density functional, M11plus, which contains nonlocal rung-3.5 correlation. We also find a good agreement between theory and experiment for some functionals without empirical dispersion corrections such as M06, r^{2}SCAN, M06-L, and revM11, as well as good performance for some functionals with added dispersion corrections such as ωB97X-D (which always has a correction) and BLYP, B3LYP, CAM-B3LYP, and PBE0 when the optional dispersion corrections are added.

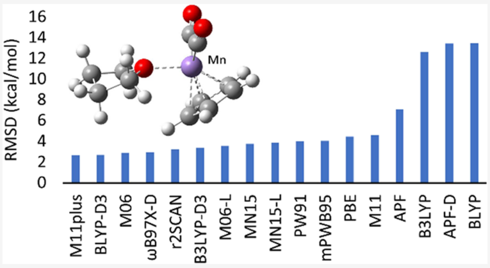

1. INTRODUCTION

An important aspect of recent advances in density functional theory (DFT) has been validating its predictions against physical quantities of known values, e.g., bond distances, bond enthalpies, heats of formation, and excitation energies. For a gateway into this enormous literature, see the GMTKN55 paper[1] and the CF22D paper[2] and the extensive references therein. The target data in the test sets used for such validation typically come from experiments; however, sometimes they come from high-level calculations. Very often DFT has been shown to give excellent agreement with the target values, justifying DFT's widespread use for a variety of applications.

Two of the authors of the present paper and a co-worker have previously compiled a set of experimental enthalpies of activation for solution-phase metal–ligand bond dissociation of 30 metal–ligand complexes (see Figure 1 and Table 1).[3] This was compared to density functional enthalpies of reaction for the bond-dissociation reactions. Although these quantities are not the same, there was an expectation that they are comparable, and this kind of comparison provides a test of whether DFT thermodynamic predictions agree with the experimental thermochemical kinetics data. In the present article, we continue this kind of comparison with additional density functionals for 30 metal–ligand complexes, and we also consider the effects of frozen versus optimized geometries, of solvation models, and of dispersion corrections. We also look at the worst cases (the largest deviation between theory and experiment) because identifying pathological cases can be as important for validation as the consideration of average errors. A special focus of the present benchmark study is the inclusion of the M11plus functional,[4] an empirically parametrized functional that contains nonlocal rung-3.5 correlation,[5,6] an ingredient not present in the other functionals tested in this work.

A vast majority of experiments producing the enthalpies of activation for dissociative displacement of photolytically generated organometallic complexes were conducted by the Bengali group at Texas A&M University at Qatar, with a few additional measurements following the same protocol from earlier work. The test set comprising 30 complexes is shown in Figure 1, which establishes the nomenclature for identifying the systems, with a letter for the complex and a number for the

Received: July 18, 2023
Revised: October 15, 2023
Accepted: October 15, 2023
Published: November 8, 2023

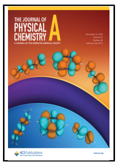

https://doi.org/10.1021/acs.jpca.3c04838
J. Phys. Chem. A 2023, 127, 9695–9704

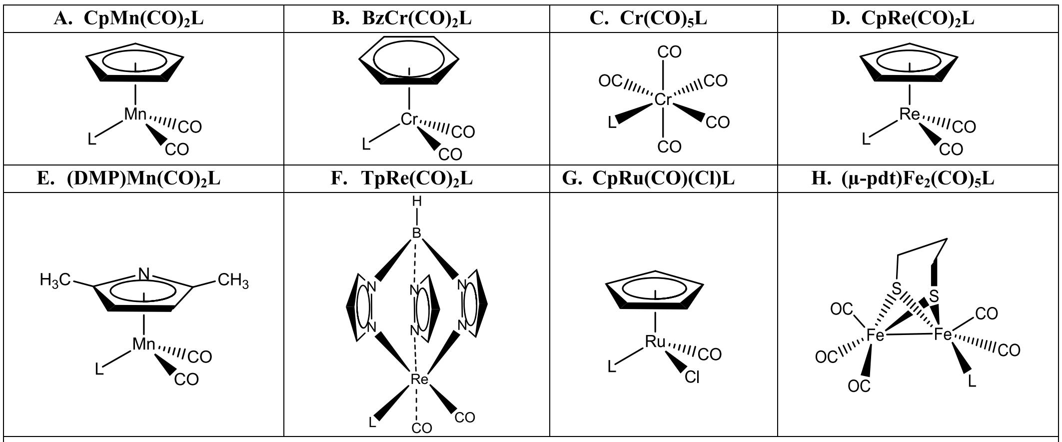

Complexes:

A01. L = η^2-2,3-dihydrofuran
A02. L = chloropropane
A03. L = η^2-cycloheptene
A04. L = η^2 -cyclooctene
A05. L = η^2-furan
A06. L = S(*n*-But)$_2$
A07. L = tetrahydrothiophene
A08. L = tetrahydrofuran (THF)
A09. L = thiophene
A10. L = toluene
A11. L = triethyl silane (TES)
B12. L = η^2-2,3-dihydrofuran
B13. L = η^2-3-hexyne
B14. L = η^2-benzene
B15. L = TES
B16. L = THF
C17. L = η^2-benzene
C18. L = η^2-3-hexyne
D19. L = heptane
E20. L = THF
E21. L = η^2-benzene
E22. L = 1-bromohexane
F23. L = THF
G24. L = η^2-cyclopentene
G25. L = η^2-cylcohexene
G26. L = η^2-cyclooctene
G27. L = THF
H28. L = η^2-3-hexyne
H29. L = η^2-cyclohexene
H30. L = η^2-2,3-dihydrofuran

Figure 1. Test set. All enthalpies of activation are for the separation of the ligand (L = 1, 2,...,30) from the complex (CL = A, B,...,H) in the reaction CL → C + L and are positive numbers. The specific target values are in Table 1 and the Supporting Information [full forms of ligand acronyms: Cp = cyclopentadienyl, Bz = benzene, DMP = 2,5-dimethylpyrrole, Tp = trispyrazolylborate, and μ-pdt = propane-1,3-dithiolate].

Table 1. Experimental Activation Energy (kcal/mol) and Solvent Used in Experiments for All Complexes in the Test Suite

name	complex (CL)	ligand (L)	experimental activation energy	solvent	ref
A01	CpMn(CO)$_2$L	η^2-2,3-dihydrofuran	28.4 ± 1.0	cyclohexane	7
A02	CpMn(CO)$_2$L	chloropropane	16.0 ± 0.6	dichloromethane	8
A03	CpMn(CO)$_2$L	η^2-cycloheptene	28.5 ± 0.8	methylcyclohexane	9
A04	CpMn(CO)$_2$L	η^2-cyclooctene	34.9 ± 0.7	methylcyclohexane	9
A05	CpMn(CO)$_2$L	η^2-furan	21.9 ± 1.0	cyclohexane	7
A06	CpMn(CO)$_2$L	S(*n*-But)$_2$	36.0 ± 1.0	methylcyclohexane	10
A07	CpMn(CO)$_2$L	tetrahydrothiophene	37.0 ± 1.0	heptane	10
A08	CpMn(CO)$_2$L	tetrahydrofuran (THF)	24.0 ± 3.0	THF	11
A09	CpMn(CO)$_2$L	thiophene	19.5 ± 2.0	heptane	3
A10	CpMn(CO)$_2$L	toluene	14.2 ± 0.8	heptane	12
A11	CpMn(CO)$_2$L	triethyl silane (TES)	27.4 ± 0.8	heptane	13
B12	BzCr(CO)$_2$L	η^2-2,3-dihydrofuran	21.0 ± 1.0	cyclohexane	7
B13	BzCr(CO)$_2$L	η^2-3-hexyne	22.8 ± 0.4	heptane	14
B14	BzCr(CO)$_2$L	η^2-benzene	11.5 ± 0.9	benzene	15
B15	BzCr(CO)$_2$L	TES	24.3 ± 1.2	heptane	16
B16	BzCr(CO)$_2$L	THF	21.4 ± 0.8	THF	16
C17	Cr(CO)$_5$L	η^2-benzene	11.4 ± 1.1	benzene	17
C18	Cr(CO)$_5$L	η^2-3-hexyne	18.3 ± 0.7	heptane	14
D19	CpRe(CO)$_2$L	heptane	13.7 ± 0.2	heptane	18
E20	(DMP)MnCO)$_2$L	THF	22.1 ± 0.5	cyclohexane	19
E21	(DMP)MnCO)$_2$L	η^2-benzene	14.9 ± 1.4	cyclohexane	19
E22	(DMP)Mn(CO)$_2$L	1-bromohexane	21.1 ± 0.4	cyclohexane	19
F23	TpRe(CO)$_2$L	THF	23.9 ± 0.9	THF	20
G24	CpRu(CO)(Cl)L	η^2-cyclopentene	18.8 ± 1.1	THF	21
G25	CpRu(CO)(Cl)L	η^2-cylcohexene	17.2 ± 1.4	THF	21
G26	CpRu(CO)(Cl)L	η^2-cyclooctene	21.0 ± 0.6	THF	21
G27	CpRu(CO)(Cl)L	THF	13.7 ± 0.3	THF	21
H28	(μ-pdt)Fe$_2$(CO)$_5$L	η^2-3-hexyne	20.9 ± 0.4	cyclohexane	22
H29	(μ-pdt)Fe$_2$(CO)$_5$L	η^2-cyclohexene	19.7 ± 0.6	cyclohexane	22
H30	(μ-pdt)Fe$_2$(CO)$_5$L	η^2-2,3-dihydrofuran	20.9 ± 1.6	cyclohexane	22

ligand that detaches; e.g., "A08" denotes the detachment of tetrahydrofuran (THF) from CpMn(CO)$_2$(THF). Table 1 continues presenting details about the test set by showing the individual references for each value and the experimental uncertainties for all target values, as well as listing the solvent used for each experimental result.

Prior to the 2016 paper,[3] one of the authors published an experimental test set of transition-metal compounds in 2013,[23] and in 2014 and 2018,[24,25] Reiher et al. published a test set using experimental ligand dissociation energies gathered from the literature. There have also been previous tests against experimental and computationally derived best estimates.[2,26] A full review of the literature of DFT being applied to transition-metal complexes would be several times longer than this paper, but it is worth noting that much of the previous work has focused on two-atom systems (discussed in ref 3). There have been two recent papers that deal with larger metal−ligand systems,[27,28] but the larger point to be made here is that this kind of chemistry is a less well studied area of DFT prediction efficacy than (say) organic enthalpies of formation, and it deserves further study.

The theoretical procedure used here differs from that used in the 2016 paper.[3] In the original study, the M06[29] functional was used to optimize the geometries because it was found to have the lowest overall deviations from experiments. In the present study, geometries were reoptimized for several functionals, including some functionals not available when the original work was published. Additional differences between the present study and the previous studies are described in Section 2.

2. COMPUTATIONAL DETAILS

All calculations were done in a development version[30] of the *Gaussian* software using program defaults, except as noted. Generalized internal coordinates (GICs), a facility that allows arbitrary redundant internal coordinates to be defined and chosen for optimization constraints and other purposes, were used. The "superfine" integration grid was used in all calculations, and we used the def2-TZVPP basis set,[31] which should be sufficient to avoid significant errors due to basis set incompleteness. All of the species (the overall system CL, the ligand L, and the complex C obtained after breaking the C-L bond) calculated in this work are neutral and in a singlet spin state. Stability calculations performed on the wave function optimized with the M06 functional and a smaller basis set indicate no instabilities for these complexes.

Single-point energies are denoted $X//Y$, which means that method Y was used to optimize geometries and calculate vibrational contributions to the enthalpy, and the energy was calculated by method X at the method-Y geometry. Rows of tables without // use consistently optimized geometries, i.e., $X = Y$.

Solvation energies were evaluated using the SMD solvation model[32] with the density functional used to optimize the geometry, e.g., to include solvation in r^{2}SCAN[33]//M06 calculations, we subtracted the gas-phase M06 energies from M06/SMD results and then added the difference to the r^{2}SCAN gas-phase energies. A brief comparison of SMD and IEFPCM solvation method[34] is included below.

The differences between this study and previous work are as follows: First, some structures have been refined because we have now found lower-energy conformations by conformational sampling. Second, because the experimental enthalpies of activation come from an analysis in which they are assumed to be independent of temperature, all enthalpies of reaction were evaluated at a single temperature, which we take here to be 0 K. Third, except in one preliminary comparison, solvation was always included.

Table 2. Density Functionals Tested

functional	ref(s)	reason included
	local functionals	
gradient approximations		
BLYP	35,36	historically popular
PW91	39	performed well previously
PBE	42	popular
gradient approximations with empirical dispersion corrections		
BLYP-D3	35,36,46	test the effect of D3
BLYP-D3(BJ)	35,36,51	test the effect of D3(BJ)
PW91-D3(BJ)	39,51	test the effect of D3(BJ)
PBE-D3	42,46	test the effect of D3
PBE-D3(BJ)	42,51	test the effect of D3(BJ)
local meta functionals		
mPWB95	40,41	performed well previously
M06-L	43	performed well previously
MN15-L	44	not tested previously
r^{2}SCAN	33	not tested previously
	hybrid functionals	
global hybrid functionals		
APF	45	performed well previously
B3LYP	37,38	popular
PBE0	52	popular
BMK	53	test effect of large HF %
mPW1B95	54	not tested previously
B1B95	55	midperformer previously
PW6B95	56	not tested previously
M06	29	top performer previously
M06-2X	29	test effect of large HF %
MN15	50	not tested previously
range-separated hybrid functionals		
CAM-B3LYP	57	midperformer previously
M11	48	for comparison to M11plus
revM11	58	for comparison to M11plus
global hybrid functionals with empirical dispersion corrections		
APF-D	45	test this dispersion correction
B3LYP-D3	37,38,46	test the effect of D3
B3LYP-D3(BJ)	37,38,51	test the effect of D3(BJ)
PBE0-D3	52,46	test the effect of D3
PBE0-D3(BJ)	52,51	test the effect of D3(BJ)
BMK-D3	53,46	test the effect of D3
BMK-D3(BJ)	53,51	test the effect of D3(BJ)
mPW1B95-D3	54,46	test the effect of D3
mPW1B95-D3(BJ)	54,51	test the effect of D3(BJ)
B1B95-D3	55,46	test the effect of D3
B1B95-D3(BJ)	55,51	test the effect of D3(BJ)
range-separated hybrid functionals with empirical dispersion corrections		
CAM-B3LYP-D3	57,46	test the effect of D3
CAM-B3LYP-D3(BJ)	57,51	test the effect of D3(BJ)
ωB97X-D	47	performed well previously
range-separated hybrid functional with nonlocal rung-3.5 correlation		
M11plus	4,49	not tested previously
doubly hybrid functional		
B2PLYP	59	completeness
doubly hybrid functionals with empirical dispersion correction		
B2PLYP-D	59,60	test the effect of D2
B2PLYP-D3	59,46	test the effect of D3(BJ)

In reporting the deviations of the calculated enthalpies of reaction from the experimental enthalpies of activation, we use the following notation:

Table 3. Deviations (kcal/mol) of Calculated Metal−Ligand Enthalpies of Dissociation from Experimental Enthalpies of Activation

	gas-phase					solvated				
method	MSD	MUD	RMSD	MaxD	worst	MSD	MUD	RMSD	MaxD	worst
ωB97X-D	0.20	1.72	2.41	6.60	**F23**	−2.06	2.42	3.16	−8.22	**A07**
r^2SCAN	3.50	3.51	4.04	7.30	**A01**	1.03	2.47	3.09	−8.01	**F23**
M06	0.58	1.54	1.91	3.72	**F23**	−1.58	2.29	2.91	−7.89	**F23**
M11	−0.68	2.41	3.31	−8.37	**A07**	−2.98	3.73	4.37	−10.17	**A04**
M11plus	3.03	3.27	3.73	7.78	**F23**	0.93	1.99	2.55	5.64	**C18**

MSD: mean signed deviation, where negative means underestimation of the target value
MUD: mean unsigned deviation
RMSD: root-mean-square deviation
MaxD: signed deviation of the maximum absolute deviation
Worst: identity of the molecule with largest |MaxD|

The set of functionals tested includes M11plus, popular functionals, functionals that did well in the previous study,[3] functionals not previously tested, and functionals with empirical damped-dispersion corrections. The functionals tested are listed in Table 2 along with their references 29, 33, 35−60 and a brief explanation of why they were included.

3. RESULTS AND DISCUSSION

The Cartesian coordinates for all of the systems, the calculated results, and the experimental target values are in the Supporting Information.

Table 4. Deviations (kcal/mol) of Calculated Metal−Ligand Enthalpies of Dissociation from Experimental Enthalpies of Activation

	M06		M11		M11Plus	
deviation	SMD	default IEFPCM	SMD	default IEFPCM	SMD	default IEFPCM
MSD	−1.58	−0.78	−2.98	−2.18	0.93	1.67
MUD	2.29	1.59	3.73	3.00	1.99	2.19
RMSD	2.91	1.96	4.37	3.73	2.55	2.61
MaxD	−7.89	−4.77	−10.17	−9.46	5.64	5.18
worst	**F23**	**A04**	**A04**	**A07**	**C18**	**C18**

We first considered gas-phase results obtained with consistently optimized geometries. These results are in Table 3. The M06 and ωB97X-D functionals appeared in the previous paper; the values presented here are slightly changed compared to that work because, in several cases, a lower-energy geometry was found for the ligand, the complex without the ligand, or the bound pair, meaning the ligand dissociation energy could be changed to a higher or lower value, and in addition to that, we are using zero-point energy (ZPE) corrections (which yield 0 K enthalpies) in place of finite-temperature enthalpies used in the previous work.

In Table 3, the "worst" complex is the same (**F23**) for three of the five functionals, and it is also the largest complex in the test set. (This difference is commented on more later, following the "fixed geometry" test.)

For the gas-phase tests in Table 3, the M06 functional has the smallest MUD, RMSD, and MaxD, while ωB97X-D has the second smallest. In addition, M11 and M11plus have similar performances, although they have a sign difference for the maximum outlier; this is discussed below. The r^2SCAN functional has the largest MUD and RMSD. The gas-phase calculations in Table 3 are less appropriate for comparison to the solution-phase experiments than all the other calculations in this paper because all the other calculations include solvation, but they are included primarily for comparison to the solvated results to show whether inclusion of solvation changes the conclusions.

The solvated results in Table 3 differ significantly from the gas-phase results; for example, M11plus now has a lower MUD and RMSD than M06. More specifically, in the gas phase, the errors are in the order M06 < ωB97X-D < M11 < M11plus < r^2SCAN, while solvent corrections change the order to M11plus < r^2SCAN ≅ M06 ≅ ωB97X-D < M11. This shows the importance of including solvation, and thus the rest of the results in this paper include solvation.

The question then becomes which solvation method to choose. The SMD solvent model was specifically parametrized to reproduce solvation-free energies accurately, and due to this, it has been used in the previous study for this test set.[3] Although the *Gaussian* manual recommends SMD for calculating free energies of solvation, the *Gaussian* default solvation method[34] is different, and it was tested; the results are shown in Table 4. Using the default IEFPCM method changes the MSE by 0.7−0.8 kcal/mol and modifies all related statistical values. Because the use of the SMD method for solvation-free energies is well validated, we will use the SMD method for testing the density functionals presented in the rest of this paper.

Table 5 shows the effect of changing the geometry. Looking across any row, one can see that the values change very little. We conclude that the ligand dissociation enthalpies are not sensitive to the geometry at which the zero-point energies and electronic energies are calculated. It is therefore acceptable to consider a basket of functionals using fixed geometries. Tables 6−8 contain the primary results of this study. In keeping with the previous work,[3] we comment here on the results obtained with M06 geometries (Table 6), although the conclusions would be the same if the M11plus geometries were used (Table 7) and only slightly different if M11 geometries were used (Table 8).

Table 6 shows that the vast majority of local functionals have the same worst case (**F23**), which is also the largest complex considered; size-dependent errors are well-known for DFT. Another large complex, **A04**, also is the first or second worst complex for many functionals, but the trend is not particularly clear beyond those two systems, and more generally, we find that different functionals have problems with different systems. When one considers all the functionals, there is no single outlier complex that functionals failed to model effectively, which could have indicated an error in the experiments or a case where the potential energy along the dissociation path is significantly nonmonotonic. We also considered the second or

Table 5. Root-Mean-Square Deviation (RMSD, kcal/mol) of Ligand Dissociation Enthalpies from Experimental Enthalpies of Activation

method	X = M06	X = M11	X = M11plus
local functionals			
BLYP//X	13.45	14.13	14.23
BLYP-D3//X	2.71	3.10	3.08
BLYP-D3(BJ)//X	3.23	3.51	3.24
PW91//X	4.01	4.75	4.25
PW91-D3(BJ)//X	4.34	4.22	4.24
PBE//X	4.47	5.25	4.74
PBE-D3//X	4.59	4.40	4.47
PBE-D3(BJ)//X	5.55	5.35	5.45
mPWB95//X	4.06	4.54	4.16
M06-L//X	3.55	3.72	3.62
MN15-L//X	3.90	3.70	3.87
r^{2}SCAN//X	3.23	3.27	3.20
global hybrid functionals			
B3LYP//X	12.61	13.17	13.18
B3LYP-D3//X	3.41	3.69	3.67
B3LYP-D3(BJ)//X	2.87	3.14	2.93
PBE0//X	5.59	6.27	5.74
PBE0-D3//X	3.12	2.97	2.99
PBE0-D3(BJ)//X	3.65	3.51	3.55
BMK	7.73	8.28	8.01
BMK-D3//X	3.96	3.75	3.89
BMK-D3(BJ)//X	4.22	3.99	4.07
mPW1B95//X	4.45	4.82	4.4
mPW1B95-D3//X	3.76	3.6	3.8
mPW1B95-D3(BJ)//X	3.77	3.65	3.77
B1B95//X	6.35	6.78	6.34
B1B95-D3//X	4.47	4.32	4.56
B1B95-D3(BJ)//X	5.36	5.25	5.44
PW6B95//X	5.41	5.72	5.41
APF//X	7.04	7.77	7.27
APF-D//X	13.42	13.43	13.00
M06//X	2.91[a]	3.29	3.01
M06-2X//X	5.96	5.91	6.17
MN15//X	3.76	3.48	3.80
range-separated hybrid functionals			
CAM-B3LYP//X	9.38	9.85	9.7
CAM-B3LYP-D3//X	3.24	3.41	3.3
CAM-B3LYP-D3(BJ)//X	3.23	3.48	3.31
ωB97X-D//X	2.94	3.15	2.98
M11//X	4.59	4.37[a]	4.52
revM11//X	3.17	3.26	3.05
M11plus//X	2.65	2.48	2.55[a]
doubly hybrid functionals			
B2PLYP//X	4.15	4.19	4.27
B2PLYP-D//X	8.91	7.94	8.95
B2PLYP-D3//X	8.15	7.31	8.18

[a] Energy and geometry from the same method.

third worst-modeled complexes, but there is still no common outlier. This provides some support for the argument that this is a valid and useful test set for comparing density functionals. Although we are comparing calculated enthalpies of reaction to experimental enthalpies of activation, we conclude from the above considerations that large MUDs and RMSDs (for example, MUDs larger than 4 kcal/mol) probably indicate a deficiency of the functional rather than a deficiency of the test protocol.

Table 6. Deviations (kcal/mol) of Ligand Dissociation Enthalpies from Experimental Enthalpies of Activation with M06 Geometries

method	MSD	MUD	RMSD	MaxD	worst
local functionals					
BLYP//M06	−13.10	13.10	13.45	−18.84	**F23**
BLYP-D3//M06	−1.36	2.13	2.71	−7.66	**F23**
BLYP-D3(BJ)//M06	0.57	2.44	3.23	−9.66	**F23**
PW91//M06	−2.42	3.10	4.01	−12.70	**F23**
PW91-D3(BJ)//M06	2.59	3.71	4.34	−8.14	**F23**
PBE//M06	−3.01	3.53	4.47	−13.62	**F23**
PBE-D3//M06	2.95	3.99	4.59	8.71	**A11**
PBE-D3(BJ)//M06	3.91	4.89	5.55	10.36	**A11**
mPWB95//M06	−2.20	3.07	4.06	−12.90	**F23**
M06-L//M06	−2.53	2.82	3.55	−8.38	**F23**
MN15-L//M06	1.92	3.48	3.90	−6.83	**F23**
r^{2}SCAN//M06	1.22	2.63	3.23	−7.91	**F23**
global hybrid functionals					
B3LYP//M06	−12.27	12.27	12.61	−19.31	**A04**
B3LYP-D3//M06	−2.59	2.95	3.41	−8.63	**A04**
B3LYP-D3(BJ)//M06	−0.85	2.09	2.87	−8.61	**F23**
PBE0//M06	−4.91	4.91	5.59	−12.97	**F23**
PBE0-D3//M06	1.26	2.70	3.12	−6.74	**F23**
PBE0-D3(BJ)//M06	1.83	3.10	3.65	−7.73	**F23**
BMK//M06	−7.15	7.15	7.73	−13.29	**A04**
BMK-D3//M06	2.31	3.31	3.96	7.19	**C18**
BMK-D3(BJ)//M06	2.61	3.61	4.22	8.20	**C17**
mPW1B95//M06	−3.47	3.56	4.45	−11.59	**F23**
mPW1B95-D3//M06	2.04	3.32	3.76	−6.47	**F23**
mPW1B95-D3(BJ)//M06	1.9	3.28	3.77	−7.6	**F23**
B1B95//M06	−5.72	5.72	6.35	−13.52	**F23**
B1B95-D3//M06	2.95	3.97	4.47	7.51	**G24**
B1B95-D3(BJ)//M06	3.79	4.75	5.36	9.02	**C17**
PW6B95//M06	−4.73	4.73	5.41	−11.38	**F23**
APF//M06	−6.55	6.55	7.04	−14.44	**F23**
APF-D//M06	12.20	12.20	13.42	24.27	**G24**
M06	−1.58	2.29	2.91	−7.89	**F23**
M06-2X//M06	−4.51	5.06	5.96	−13.58	**A04**
MN15//M06	2.66	3.33	3.76	6.94	**C18**
range-separated hybrid functionals					
CAM-B3LYP//M06	−8.94	8.94	9.38	−15.94	**A04**
CAM-B3LYP-D3//M06	−2.16	2.76	3.24	−8.42	**A04**
CAM-B3LYP-D3(BJ)//M06	−2.00	2.77	3.23	−8.8	**A04**
ωB97X-D//M06	−1.82	2.28	2.94	−7.16	**A04**
M11//M06	−3.12	3.96	4.59	−10.41	**A04**
revM11//M06	−1.71	2.46	3.17	−6.83	**A04**
M11plus//M06	0.98	2.14	2.65	5.81	**C18**
doubly hybrid functionals					
B2PLYP//M06	0.97	3.45	4.15	−8.59	**F23**
B2PLYP-D//M06	7.67	7.74	8.91	15.86	**A11**
B2PLYP-D3//M06	6.78	7.13	8.15	15.56	**A11**

There are many functionals that do quite well, with RMSD < 3.7 kcal/mol, and these are either modern functionals (M11plus, revM11, M06-L, ωB97X-D, r^{2}SCAN) or older hybrid functionals with dispersion corrections (BLYP, B3LYP, CAM-B3LYP, PBE0). Adding a dispersion correction greatly improves BLYP, PBE0, CAM-B3LYP, and B3LYP, for which the dispersion terms are added without reparametrizing the rest of the functional; ωB97X-D, which has an empirical dispersion correction that is included in the functional during

Table 7. Deviations (kcal/mol) of Ligand Dissociation Enthalpies from Experimental Enthalpies of Activation with M11 Geometries

method	MSD	MUD	RMSD	MaxD	worst
local functionals					
BLYP//M11	−13.72	13.72	14.13	−20.88	**F23**
BLYP-D3//M11	−1.70	2.45	3.10	−8.73	**F23**
BLYP-D3(BJ)//M11	0.23	2.75	3.51	−10.88	**F23**
PW91//M11	−3.18	3.89	4.75	−14.38	**F23**
PW91-D3(BJ)//M11	1.9	3.37	4.22	−9.53	**F23**
PBE//M11	−3.78	4.36	5.25	−15.27	**F23**
PBE-D3//M11	2.28	3.61	4.4	−8.70	**F23**
PBE-D3(BJ)//M11	3.27	4.46	5.35	10.40	**A11**
mPWB95//M11	−2.72	3.64	4.54	−14.13	**F23**
M06-L//M11	−2.72	2.94	3.72	−9.06	**F23**
MN15-L//M11	1.77	3.25	3.70	−6.88	**F23**
r^2SCAN//M11	0.63	2.56	3.27	−9.08	**F23**
global hybrid functionals					
B3LYP//M11	−12.82	12.82	13.17	−19.09	**A04**
B3LYP-D3//M11	−2.90	3.18	3.69	−8.50	**A04**
B3LYP-D3(BJ)//M11	−1.18	2.41	3.14	−9.73	**F23**
PBE0//M11	−5.63	5.63	6.27	−14.47	**F23**
PBE0-D3//M11	0.68	2.50	2.97	−7.83	**F23**
PBE0-D3(BJ)//M11	1.23	2.85	3.51	−8.85	**F23**
BMK//M11	−7.76	7.76	8.28	−13.40	**A04**
BMK-D3//M11	2.01	3.11	3.75	7.80	**C18**
BMK-D3(BJ)//M11	2.18	3.33	3.99	9.42	**C18**
mPW1B95//M11	−3.93	4.00	4.82	−12.64	**F23**
mPW1B95-D3//M11	1.75	3.11	3.6	−7.08	**F23**
mPW1B95-D3(BJ)//M11	1.52	3.05	3.65	−8.40	**F23**
B1B95//M11	−6.20	6.20	6.78	−14.64	**F23**
B1B95-D3//M11	2.74	3.79	4.32	7.15	**C18**
B1B95-D3(BJ)//M11	3.50	4.47	5.25	9.51	**C18**
PW6B95//M11	−5.10	5.10	5.72	−12.41	**F23**
APF//M11	−7.28	7.28	7.77	−16.05	**F23**
APF-D//M11	12.30	12.31	13.43	23.94	**G24**
M06//M11	−2.20	2.62	3.29	−8.79	**F23**
M06-2X//M11	−4.45	4.89	5.91	−13.42	**A04**
MN15//M11	2.30	2.99	3.48	6.63	**C18**
range-separated hybrid functionals					
CAM-B3LYP//M11	−9.44	9.44	9.85	−15.83	**A04**
CAM-B3LYP-D3//M11	−2.48	2.92	3.41	−8.37	**A04**
CAM-B3LYP-D3(BJ)//M11	−2.39	3.02	3.48	−8.77	**A04**
*ω*B97X-D//M11	−2.28	2.53	3.15	−7.29	**A04**
M11	−2.98	3.73	4.37	−10.17	**A04**
revM11//M11	−2.08	2.62	3.26	−7.28	**F23**
M11plus//M11	0.54	1.92	2.48	5.33	**C18**
doubly hydrid functionals					
B2PLYP//M11	−0.29	3.38	4.19	−10.10	**F23**
B2PLYP-D//M11	6.54	6.70	7.94	15.85	**A11**
B2PLYP-D3//M11	5.64	6.15	7.31	15.48	**A11**

Table 8. Deviations (kcal/mol) of Ligand Dissociation Enthalpies from Experimental Enthalpies of Activation with M11plus Geometries

method	MSD	MUD	RMSD	MaxD	worst
local functionals					
BLYP//M11plus	−13.85	13.85	14.23	−19.77	**F23**
BLYP-D3//M11plus	−1.86	2.44	3.08	−7.89	**F23**
BLYP-D3(BJ)//M11plus	0.16	2.49	3.24	−10.00	**F23**
PW91//M11plus	−2.69	3.36	4.25	−13.17	**F23**
PW91-D3(BJ)//M11plus	2.38	3.60	4.24	−8.40	**F23**
PBE//M11plus	−3.30	3.82	4.74	−14.11	**F23**
PBE-D3//M11plus	2.74	3.85	4.47	7.95	**A11**
PBE-D3(BJ)//M11plus	3.77	4.80	5.45	9.67	**A11**
mPWB95//M11plus	−2.28	3.19	4.16	−13.16	**F23**
M06-L//M11plus	−2.57	2.87	3.62	−8.18	**F23**
MN15-L//M11plus	2.02	3.42	3.87	−6.33	**F23**
r^2SCAN//M11plus	1.14	2.57	3.20	−7.94	**F23**
global hybrid functionals					
B3LYP//M11plus	−12.84	12.84	13.18	−19.55	**A04**
B3LYP-D3//M11plus	−2.95	3.24	3.67	−8.75	**A04**
B3LYP-D3(BJ)//M11plus	−1.15	2.17	2.93	−8.73	**F23**
PBE0//M11plus	−5.10	5.10	5.74	−13.21	**F23**
PBE0-D3//M11plus	1.18	2.57	2.99	−6.66	**F23**
PBE0-D3(BJ)//M11plus	1.76	2.98	3.55	−7.70	**F23**
BMK//M11plus	−7.47	7.47	8.01	−13.39	**A04**
BMK-D3//M11plus	2.27	3.26	3.89	7.21	**C18**
BMK-D3(BJ)//M11plus	2.46	3.48	4.07	8.33	**C17**
mPW1B95//M11plus	−3.44	3.55	4.40	−11.57	**F23**
mPW1B95-D3//M11plus	2.22	3.35	3.80	6.47	**B12**
mPW1B95-D3(BJ)//M11plus	2.00	3.28	3.77	−7.41	**F23**
B1B95//M11plus	−5.74	5.74	6.34	−13.55	**F23**
B1B95-D3//M11plus	3.17	4.04	4.56	7.27	**B12**
B1B95-D3(BJ)//M11plus	3.97	4.81	5.44	9.57	**C17**
PW6B95//M11plus	−4.77	4.77	5.41	−11.38	**F23**
APF//M11plus	−6.80	6.80	7.27	−14.77	**F23**
APF-D//M11plus	11.99	11.99	13.00	21.74	**G26**
M06//M11plus	−1.79	2.43	3.01	−7.65	**F23**
M06-2X//M11plus	−4.80	5.22	6.17	−13.86	**A04**
MN15//M11plus	2.78	3.33	3.80	6.86	**C18**
range-separated hybrid functionals					
CAM-B3LYP//M11plus	−9.29	9.29	9.70	−15.98	**A04**
CAM-B3LYP-D3//M11plus	−2.35	2.86	3.30	−8.38	**A04**
CAM-B3LYP-D3(BJ)//M11plus	−2.24	2.87	3.31	−8.79	**A04**
*ω*B97X-D//M11plus	−2.06	2.36	2.98	−7.14	**A04**
M11//M11plus	−3.16	3.89	4.52	−10.38	**A04**
revM11//M11plus	−1.68	2.38	3.05	−6.50	**A04**
M11plus	0.93	1.99	2.55	5.64	**C18**
doubly hybrid functionals					
B2PLYP//M11plus	0.84	3.59	4.27	−8.76	**F23**
B2PLYP-D//M11plus	7.72	7.78	8.95	16.43	**A03**
B2PLYP-D3//M11plus	6.78	7.13	8.18	15.04	**A11**

its original optimization, also gives good results. The effectiveness of dispersion corrections for modeling organometallic compounds has been studied elsewhere,[26] and these corrections generally improve the accuracy of most functionals. It is well known that the efficacy of some empirically corrected functionals arises not from getting dispersion right but rather because the correction acts more generally to cancel errors. We should keep in mind that the so-called dispersion correction only represents true dispersion at large interfragment distances;[61] at bonding distances, it is simply an empirical correction to all components of the energy (for this reason, it is probably better to call it a damped-dispersion correction or a molecular mechanics correction than to use the shorthand of calling it a dispersion correction). It should also be noted that

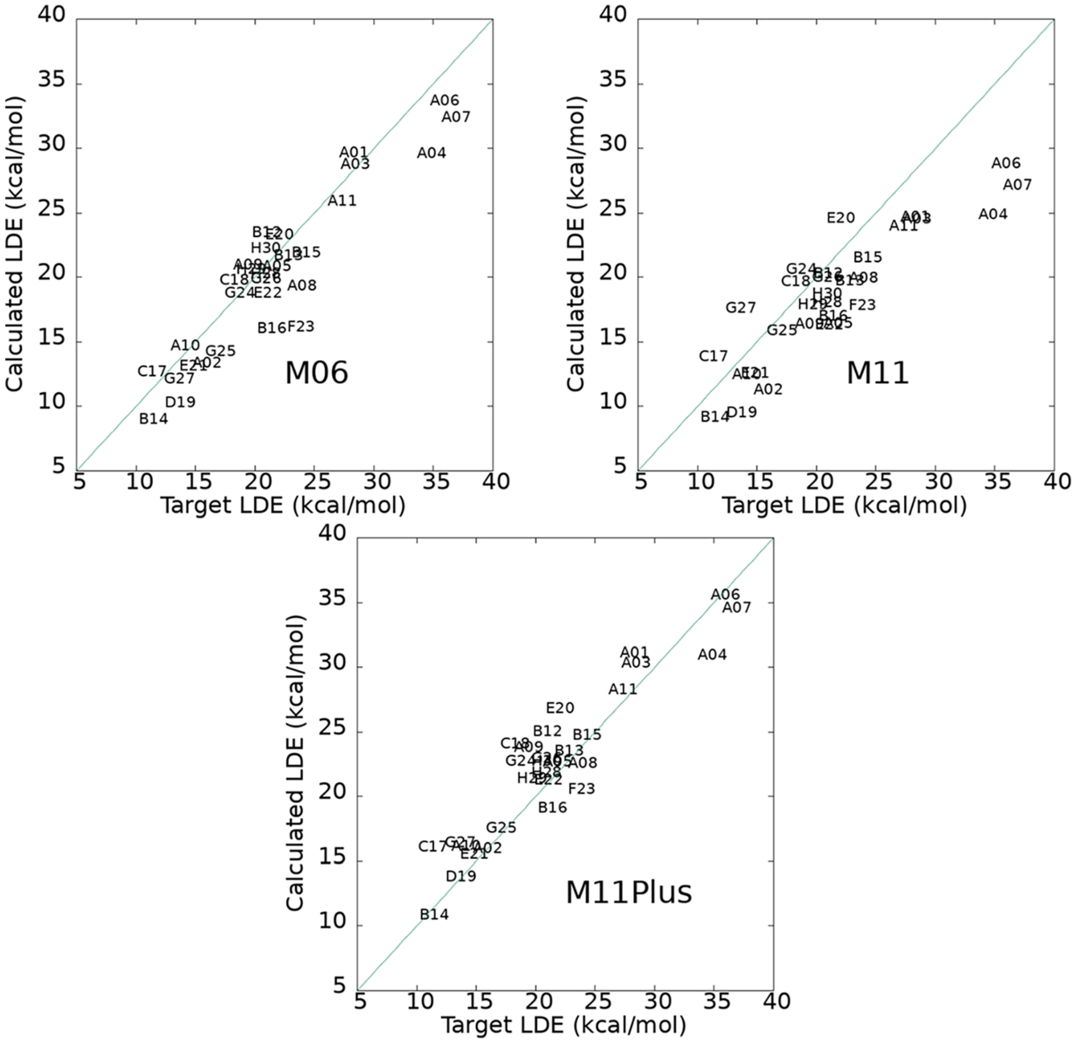

Figure 2. Calculated ligand dissociation enthalpies (LDE) plotted against target values with a perfect-agreement line to guide the eye. All geometries and energies are calculated consistently, and all points are labeled with the identity of the complex.

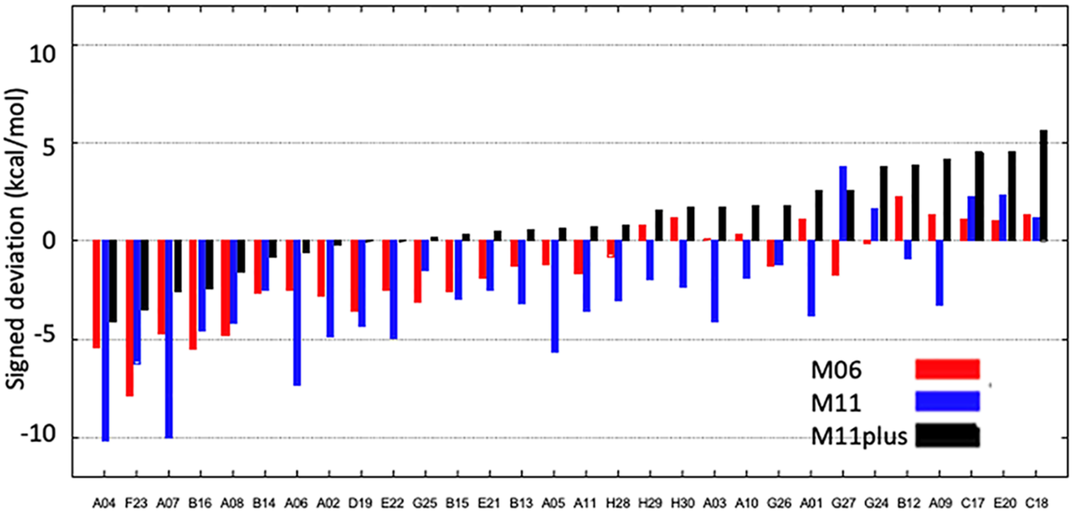

Figure 3. Signed deviations of ligand dissociation enthalpy (kcal/mol) for three functionals, M06, M11, and M11plus. The systems are ordered by the signed error of the M11plus results. All geometries and energies are calculated consistently.

there are multiple ways to dampen the dispersion correction at bonding distances, including the original D3 functional form (sometimes called D3(0)) and the Becke–Johnson (BJ) version of D3. We find that the BJ version of dispersion generally does slightly worse, and therefore, it is not recommended for these systems.

Contrary to the general benefit of dispersion corrections, adding dispersion terms to the APF functional makes the results much worse. This is unfortunate because the APF functional was originally designed to avoid spurious long-range attractions so that adding dispersion terms would be more physical. The results of APF-D deserve more study, as the results both without and with sampled dispersion terms agree less well with experiments than all the other functionals studied except BLYP and B3LYP. Since the mean signed error of APF has the same sign as that of BLYP and B3LYP, which are both improved by dispersion terms, it is likely that APF could also be improved by dispersion terms if they were reparametrized. Also deserving of more study are the doubly hybrid results obtained by applying dispersion correction to B2PLYP. The dispersion correction dramatically increases the error for B2PLYP. This is a surprising result because B2PLYP already contains some dispersion in its MP2 term, so the size of the dispersion correction should be small. (We should also keep in mind that MP2 itself often overestimates the dispersion, but the percentage of MP2 correlation in B2PLYP is only 27%, so it should still underestimate dispersion.)

The enthalpies calculated with M06 and M06-L agree better with experiments than those calculated with MN15 and MN15-L, although on broader comparison sets, the latter functionals, which were developed more recently, are usually better. It should also be noted that functionals with the original B95 correlation term generally do not perform well for this test set.

Of all the functionals studied, M11plus agrees best with experiments for this data set, especially in terms of the maximum outlier. This is a very encouraging result for the rung-3.5 correlation terms included in M11plus.

Figure 2 illustrates how M06, M11, and M11plus do not all have their best or worst agreements with the same ligand/complex pairing. The M06 results cluster around the perfect-agreement line with some significant underestimation throughout; M11 shows the same underestimation, with the deviation increasing with larger binding enthalpies; and M11plus clearly worked well throughout the range.

To better compare the three functionals, the complexes were sorted by the signed deviation of M11plus, and then the results of M06 and M11 were placed in the same order; the resulting comparison is presented in Figure 3. This figure makes it clear that the order of these deviations differs for different functionals, and that there are no common problem cases. Sometimes M06 agrees with the experiment much better than M11plus, and in some other cases M11plus agrees much better. If the data is further subdivided, by looking at the results for the most common ligand (THF) or for a single parent complex (**A**, $CpMn(CO)_2$), one still finds that the order of these deviations differs for different functionals, which further supports the diversity of the test set. Finally, examining the maximum outliers on either end of the range for M11plus reveals no common structural characteristic or ligand, i.e., the edge cases do not have something chemical in common.

4. CONCLUSIONS

In light of the situation where we are comparing calculated enthalpies of reaction to experimental enthalpies of activation, we should probably not place too much emphasis on small differences of the MUD or RMSD of functionals whose MUD is less than 4 kcal/mol. Therefore, we consider an RMSD less than 4 kcal/mol as a mark of success for agreeing well with the experimental data. With this criterion of success, we find there are two groups of functionals that are successful, namely, (i) modern functionals like M11plus, revM11, ωB97X-D, r^2SCAN, MN15, and MN15-L and (ii) traditional local and hybrid functionals with dispersion corrections like BLYP+D, B3LYP+D, CAM-B3LYP+D, and PBE0+D. It is encouraging for the efficacy of rung-3.5 correlation terms that M11plus agrees best with the experimental data.

■ ASSOCIATED CONTENT

Supporting Information

The Supporting Information is available free of charge at https://pubs.acs.org/doi/10.1021/acs.jpca.3c04838.

> Tar file containing two directories of text files: one directory with Cartesian coordinates along with naming conventions as in Figure 1 and the other with data tables of all the ligand dissociation enthalpies (ZIP)

■ AUTHOR INFORMATION

Corresponding Author

Edward N. Brothers − *Gaussian, Inc., Wallingford, Connecticut 06492, United States*; orcid.org/0000-0003-3709-7646; Email: ed@gaussian.com

Authors

Ashfaq A. Bengali − *Division of Arts and Sciences, Texas A&M University at Qatar, Doha, Qatar*; orcid.org/0000-0002-6765-8320

Giovanni Scalmani − *Gaussian, Inc., Wallingford, Connecticut 06492, United States*; orcid.org/0000-0002-4597-7195

Benjamin G. Janesko − *Department of Chemistry and Biochemistry, Texas Christian University, Fort Worth, Texas 76110, United States*; orcid.org/0000-0002-2572-5273

Pragya Verma − *Department of Chemistry, Chemical Theory Center, and Minnesota Supercomputing Institute, University of Minnesota, Minneapolis, Minnesota 55455-0431, United States*; orcid.org/0000-0002-5722-0894

Donald G. Truhlar − *Department of Chemistry, Chemical Theory Center, and Minnesota Supercomputing Institute, University of Minnesota, Minneapolis, Minnesota 55455-0431, United States*; orcid.org/0000-0002-7742-7294

Michael J. Frisch − *Gaussian, Inc., Wallingford, Connecticut 06492, United States*

Complete contact information is available at: https://pubs.acs.org/10.1021/acs.jpca.3c04838

Notes

The authors declare no competing financial interest.

■ ACKNOWLEDGMENTS

E.N.B. acknowledges A.V. Marenich for help with GIC. E.N.B. and A.A.B. acknowledge R. K. Raju for informative discussions. This work was supported in part by the National Science Foundation under grant CHE-2054723.

■ REFERENCES

(1) Goerigk, L.; Hansen, A.; Bauer, C.; Ehrlich, S.; Najibi, A.; Grimme, S. A look at the density functional theory zoo with the advanced GMTKN55 database for general main group thermochemistry, kinetics and noncovalent interactions. *Phys. Chem. Chem. Phys.* **2017**, *19*, 32184−32215.

(2) Liu, Y.; Zhang, C.; Liu, Z.; Truhlar, D. G.; Wang, Y.; He, X. Supervised learning of a chemistry functional with damped dispersion. *Nat. Comput. Sci.* **2023**, *3*, 48−58.

(3) Raju, R. K.; Bengali, A. A.; Brothers, E. N. A unified set of experimental organometallic data used to evaluate modern theoretical methods. *Dalton Trans.* **2016**, *45*, 13766−13778.

(4) Verma, P.; Janesko, B. G.; Wang, Y.; He, X.; Scalmani, G.; Frisch, M. J.; Truhlar, D. G. M11plus: A range-separated hybrid meta functional with both local and rung-3.5 correlation terms and high across-the-board accuracy for chemical applications. *J. Chem. Theory Comput.* **2019**, *15*, 4804−4815.

(5) Janesko, B. G. Rung 3.5 density functionals: Another step on Jacob's ladder. *Int. J. Quantum Chem.* **2013**, *113*, 83−88.

(6) Janesko, B. G. Replacing hybrid density functional theory: Motivation and recent advances. *Chem. Soc. Rev.* **2021**, *50*, 8470−8495.

(7) Andreatta, J. R.; Cieslinski, G. B.; Batool, M.; Sun, X.-Z.; George, M. W.; Brothers, E. N.; Darensbourg, D. J.; Bengali, A. A. Displacement kinetics of η^2-bound furan and 2,3-dihydrofuran from Mn and Cr centers: Evidence for the partial dearomatization of the furan ligand. *Inorg. Chem.* **2009**, *48*, 7787−7793.

(8) Bengali, A. A.; Fan, W. Y. Reactivity of the CpMn(CO)$_2$−XR Bond [X = Cl, Br]: A kinetic study using rapid-scan FTIR spectroscopy. *Organometallics* **2008**, *27*, 5488−5493.

(9) Angelici, R. J.; Loewen, W. Kinetic studies of olefin replacement in cyclopentadienylmanganese-olefin-dicarbonyl complexes. *Inorg. Chem.* **1967**, *6*, 682−686.

(10) Butler, I. S.; Sawai, T. Reactions of metal carbonyl complexes. VII. Kinetics and mechanism of the organosulfide substitution reactions of some (η5-cyclopentadienyl)dicarbonyl(organosulfide)-manganese(I) complexes with tertiary phosphines and phosphites. *Inorg. Chem.* **1975**, *14*, 2703−2707.

(11) Coleman, J. E.; Dulaney, K. E.; Bengali, A. A. Displacement of the THF solvent molecule from (η^5-C_5H_5)Mn(CO)$_2$THF by simple two electron donor ligands: evidence for a dissociative mechanism and determination of the Mn−THF bond strength. *J. Organomet. Chem.* **1999**, *572*, 65−71.

(12) Bengali, A. A. Observation of the (η^5-C_5H_5)Mn(CO)$_2$(toluene) complex by low-temperature IR spectroscopy and determination of the manganese−toluene bond strength. *Organometallics* **2000**, *19*, 4000−4003.

(13) Hester, D. M.; Sun, J.; Harper, A. W.; Yang, G. K. Characterization of the energy surface for the oxidative addition of silanes to manganese complex CpMn(CO)$_2$(heptane). *J. Am. Chem. Soc.* **1992**, *114*, 5234−5240.

(14) Swennenhuis, B. H. G.; Cieslinski, G. B.; Brothers, E. N.; Bengali, A. A. Reactivity of the M-(η^2-alkyne) bond [M= Cr, W]: A kinetic and DFT study. *J. Organomet. Chem.* **2010**, *695*, 891−897.

(15) Bengali, A. A.; Grunbeck, A. R. Investigating the reactivity of the (η^6-C_6H_5R)Cr(CO)$_2$−(η^2-C_6H_5R) [R = H, CH_3, CF_3] bond: A laser flash photolysis study with infrared detection. *Organometallics* **2005**, *24*, 5919−5924.

(16) Bengali, A. A.; Fehnel, R. Mechanism and energetics of silane and THF displacement from the (η^6-C_6H_6)Cr(CO)$_2$(HSiEt$_3$) and (η^6-C_6H_6)Cr(CO)$_2$(THF) complexes. *Organometallics* **2005**, *24*, 1156−1160.

(17) Bengali, A. A.; Stumbaugh, T. F. Estimating the (CO)$_5$Cr−(η^2-benzene) bond dissociation enthalpy: reaction of the (CO)$_5$Cr(η^2-benzene) complex with a series of $(CH_3)_n$THF (n = 0, 1, 2, and 4) ligands. *Dalton Trans.* **2003**, *3*, 354−360.

(18) Bengali, A. A. Displacement of the heptane solvent from (η^5-C_5H_5)Re(CO)$_2$(heptane): A flash photolysis study using infrared detection. *J. Organomet. Chem.* **2005**, *690*, 4989−4992.

(19) Swennenhuis, B. H. G.; Poland, R.; Fan, W. Y.; Darensbourg, D. J.; Bengali, A. A. Ligand substitution from the (η^5-DMP)Mn-(CO)$_2$(Solv) [DMP = 2,5-dimethylpyrrole, Solv = solvent] complexes: To ring slip or not to ring slip? *Inorg. Chem.* **2010**, *49*, 7597−7604.

(20) Bengali, A. A.; Mezick, B. K.; Hart, M. N. Electronic and steric influences on the rate and energetics of THF and Me$_n$THF (n = 1, 2) displacement from LRe(CO)$_2$ (L = Tp, Tp*, Cp*) fragments by acetonitrile. *Organometallics* **2003**, *22*, 5436−5440.

(21) Muhammad, S.; Kyran, S. J.; Raju, R. K.; Brothers, E. N.; Darensbourg, D. J.; Bengali, A. A. Time-resolved infrared spectroscopy studies of olefin binding in photogenerated CpRu(CO)X (X = Cl, I) transients. *Organometallics* **2012**, *31*, 3972−3279.

(22) Muhammad, S.; Moncho, S.; Brothers, E. N.; Darensbourg, M. Y.; Darensbourg, D. J.; Bengali, A. A. Time-resolved infrared spectroscopy studies of olefin binding in photogenerated CpRu-(CO)X (X = Cl, I) transients. *Inorg. Chem.* **2012**, *51*, 7362−7369.

(23) Zhang, W.; Truhlar, D. G.; Tang, M. Tests of exchange-correlation functional approximations against reliable experimental data for average bond energies of 3d transition metal compounds. *J. Chem. Theory Comput.* **2013**, *9*, 3965−3977.

(24) Weymuth, T.; Couzijn, E. P. A.; Chen, P.; Reiher, M. New benchmark set of transition metal coordination reactions for the assessment of density functionals. *J. Chem. Theory Comput.* **2014**, *10*, 3092−3103.

(25) Husch, T.; Freitag, L.; Reiher, M. Calculation of ligand dissociation energies in large transition-metal complexes. *J. Chem. Theory Comput.* **2018**, *14*, 2456−2468.

(26) Bursch, M.; Caldeweyher, E.; Hansen, A.; Neugebauer, H.; Ehlert, S.; Grimme, S. Understanding and quantifying London dispersion effects in organometallic complexes. *Acc. Chem. Res.* **2019**, *52*, 258−266.

(27) Grotjahn, R.; Kaupp, M. A look at real-world transition-metal thermochemistry and kinetics with local hybrid functionals. *Isr. J. Chem.* **2023**, *63*, No. e2022001.

(28) Maurer, L. R.; Bursch, M.; Grimme, S.; Hansen, A. Assessing density functional theory for chemically relevant open-shell transition metal reactions. *J. Chem. Theory Comput.* **2021**, *17*, 6134−6151.

(29) Zhao, Y.; Truhlar, D. The M06 suite of density functionals for main group thermochemistry, thermochemical kinetics, noncovalent interactions, excited states, and transition elements: Two new functionals and systematic testing of four M06-class functionals and 12 other functionals. *Theor. Chem. Acc.* **2008**, *120*, 215−241.

(30) Frisch, M. J.; Trucks, G. W.; Schlegel, H. B.; Scuseria, G. E.; Robb, M. A.; Cheeseman, J. R.; Scalmani, G.; Barone, V.; Petersson, G. A.; Nakatsuji, H. *Gaussian Development Version Revision J.24+*; Gaussian Inc.: Wallingford, CT, 2023.

(31) Weigend, F.; Ahlrichs, R. Balanced basis sets of split valence, triple zeta valence and quadruple zeta valence quality for H to Rn: Design and assessment of accuracy. *Phys. Chem. Chem. Phys.* **2005**, *7*, 3297−3305.

(32) Marenich, A. V.; Cramer, C. J.; Truhlar, D. G. Universal solvation model based on solute electron density and on a continuum model of the solvent defined by the bulk dielectric constant and atomic surface tensions. *J. Phys. Chem. B* **2009**, *113*, 6378−6396.

(33) Furness, J. W.; Kaplan, A. D.; Ning, J.; Perdew, J. P.; Sun, J. Accurate and numerically efficient r^{2}SCAN meta-generalized gradient approximation. *J. Phys. Chem. Lett.* **2020**, *11*, 8208−8215.

(34) Scalmani, G.; Frisch, M. J. Continuous surface charge polarizable continuum models of solvation. I. General formalism. *J. Chem. Phys.* **2010**, *132*, 114110.

(35) Becke, A. D. Density-functional exchange-energy approximation with correct asymptotic behavior. *Phys. Rev. A* **1988**, *38*, 3098−3100.

(36) Lee, C.; Yang, W.; Parr, R. G. Development of the Colle-Salvetti correlation-energy formula into a functional of the electron density. *Phys. Rev. B* **1988**, *37*, 785−789.

(37) Becke, A. D. Density-functional thermochemistry. III. The role of exact exchange. *J. Chem. Phys.* **1993**, *98*, 5648−5652.

(38) Stephens, P. J.; Devlin, F. J.; Chabalowski, C. F.; Frisch, M. J. Ab initio calculation of vibrational absorption and circular dichroism spectra using density functional force fields. *J. Phys. Chem.* **1994**, *98*, 11623−11627.

(39) Perdew, J. P.; Chevary, J. A.; Vosko, S. H.; Jackson, K. A.; Pederson, M. R.; Singh, D. J.; Fiolhais, C. Atoms, molecules, solids, and surfaces: Applications of the generalized gradient approximation for exchange and correlation. *Phys. Rev. B* **1992**, *46*, 6671−6687.

(40) Adamo, C.; Barone, V. Exchange functionals with improved long-range behavior and adiabatic connection methods without adjustable parameters: The mPW and mPW1PW models. *J. Chem. Phys.* **1998**, *108*, 664−675.

(41) Becke, A. D.; Density-functional thermochemistry. IV. A new dynamical correlation functional and implications for exact-exchange mixing. *J. Chem. Phys.* **1996**, *104*, 1040−1046.

(42) Perdew, J. P.; Burke, K.; Ernzerhof, M. Generalized gradient approximation made simple. *Phys. Rev. Lett.* **1996**, *77*, 3865−3868.

(43) Zhao, Y.; Truhlar, D. G. A new local density functional for main-group thermochemistry, transition metal bonding, thermochemical kinetics, and noncovalent interactions. *J. Chem. Phys.* **2006**, *125*, 194101.

(44) Yu, H. S.; He, X.; Truhlar, D. G. MN15-L: A new local exchange-correlation functional for Kohn−Sham density functional theory with broad accuracy for atoms, molecules, and solids. *J. Chem. Theory Comput.* **2016**, *12*, 1280−1293.

(45) Austin, A.; Petersson, G. A.; Frisch, M. J.; Dobek, F. J.; Scalmani, G.; Throssell, K. A density functional with spherical atom dispersion terms. *J. Chem. Theory Comput.* **2012**, *8*, 4989−5007.

(46) Grimme, S.; Antony, J.; Ehrlich, S.; Krieg, H. A consistent and accurate ab initio parametrization of density functional dispersion correction (DFT-D) for the 94 elements H-Pu. *J. Chem. Phys.* **2010**, *132*, 154104.

(47) Chai, J.-D.; Head-Gordon, M. Long-range corrected hybrid density functionals with damped atom−atom dispersion corrections. *Phys. Chem. Chem. Phys.* **2008**, *10*, 6615−6620.

(48) Peverati, R.; Truhlar, D. G. Improving the accuracy of hybrid meta-GGA density functionals by range separation. *J. Phys. Chem. Lett.* **2011**, *2*, 2810−2817.

(49) Janesko, B. G.; Verma, P.; Scalmani, G.; Frisch, M. J.; Truhlar, D. G. M11plus, a range-separated hybrid meta functional incorporating nonlocal rung-3.5 correlation, exhibits broad accuracy on diverse databases. *J. Phys. Chem. Lett.* **2020**, *11*, 3045−3050.

(50) Yu, H. S.; He, X.; Li, S. L.; Truhlar, D. G. MN15: A Kohn−Sham global-hybrid exchange−correlation density functional with broad accuracy for multi-reference and single-reference systems and noncovalent interactions. *Chem. Sci.* **2016**, *7*, 5032−5051.

(51) Grimme, S.; Ehrlich, S.; Goerigk, L. Effect of the damping function in dispersion corrected density functional theory. *J. Comput. Chem.* **2011**, *32*, 1456−65.

(52) Adamo, C.; Barone, V. Toward reliable density functional methods without adjustable parameters: The PBE0 model. *J. Chem. Phys.* **1999**, *110*, 6158−69.

(53) Boese, A. D.; Martin, J. M. L. Development of density functionals for thermochemical kinetics. *J. Chem. Phys.* **2004**, *121*, 3405−3416.

(54) Zhao, Y.; Truhlar, D. G. Hybrid meta density functional theory methods for thermochemistry, thermochemical kinetics, and noncovalent interactions: The MPW1B95 and MPWB1K models and comparative assessments for hydrogen bonding and van der Waals interactions. *J. Phys. Chem. A* **2004**, *108*, 6908−6918.

(55) Becke, A. D. Density-functional thermochemistry. IV. A new dynamical correlation functional and implications for exact-exchange mixing. *J. Chem. Phys.* **1996**, *104*, 1040−1046.

(56) Zhao, Y.; Truhlar, D. G. Design of density functionals that are broadly accurate for thermochemistry, thermochemical kinetics, and nonbonded interactions. *J. Phys. Chem. A* **2005**, *109*, 5656−5667.

(57) Yanai, T.; Tew, D. Handy N.A new hybrid exchange-correlation functional using the Coulomb-attenuating method (CAM-B3LYP). *Chem. Phys. Lett.* **2004**, *393*, 51−57.

(58) P. Verma, P.; Wang, Y.; Ghosh, S.; He, X.; Truhlar, D. G. Revised M11 exchange-correlation functional for electronic excitation energies and ground-state properties. *J. Phys. Chem. A* **2019**, *123*, 2966−2990.

(59) Grimme, S. Semiempirical hybrid density functional with perturbative second-order correlation. *J. Chem. Phys.* **2006**, *124*, No. 034108.

(60) Grimme, S. Semiempirical GGA-type density functional constructed with a long-range dispersion correction. *J. Comput. Chem.* **2006**, *27*, 1787−1799.

(61) Truhlar, D. G. Dispersion forces: Neither fluctuating nor dispersing. *J. Chem. Educ.* **2019**, *96*, 1671−1675.